Vol 18 No 8, August 2009
1674-1056/2009/18(08)/3318-07

Chinese Physics B

© 2009 Chin. Phys. Soc.
and IOP Publishing Ltd

An experiment of dynamical behaviours in an erbium-doped fibre-ring laser with loss modulation

Liu Yue(刘 越)†, Feng Xue(冯 雪), Zhang Wei(张 巍), and Liu Xiao-Ming(刘小明)

Department of Electronic Engineering, Tsinghua University, Beijing 100084, *China*

(Received 3 September 2008; revised manuscript received 13 February 2009)

This paper reports a systematic experimental investigation on the dynamics in the low-frequency region in an erbium-doped fibre-ring laser with loss modulation. A rich variety of bifurcation is analyzed through the bifurcation diagram and structured with the concept of the winding numbers. The coexistence of multiple attractors and the crisis that appear in the saddle-node bifurcations, and an interesting structure of bifurcation which is similar to the bifurcations in high-frequency range, have been observed.

Keywords: erbium-doped fibre-ring laser, bifurcation, winding number, attractor
PACC: 0545, 0547, 4255N

1. Introduction

In the last few decades, enormous progress has been achieved in the research of erbium-doped fibre lasers (EDFLs) for their wide applications in various fields, such as secure communication, sensing, spectroscopy, and medicine.[1] As the fast polarization variables can be adiabatically eliminated, EDFLs, along with solid-state, CO_2 and semiconductor lasers, are Class-B lasers. The dynamics of these lasers can be described by two rate equations for optical intensity and population inversion.[2] With additional degrees of freedom, e.g. external modulation of loss or pump,[3−7] delay feedback[8] and coupled dual rings,[7,9,10] chaos through period-doubling bifurcation, intermittency and quasi-periodic routes were observed in EDFLs.[4−10] Self-pulsing and a bistability between 2T- and 3T-period orbits were also found and analyzed in a heavily doped fiber laser.[11] Recently, the coexistence of two or more period attractors in EDFLs with parameter modulation[3−5] has been reported as was shown in a Q-switched CO_2 laser.[12] Each attractor is determined by the initial conditions and its periodicity is equal to the subharmonic or higher harmonic branches of the modulation frequency.[5] Each branch is born in regular saddle-node bifurcations (SNBs)[13] when the modulation (driving) frequency is close to the corresponding harmonic of the relaxation oscillation frequency of the laser. The overlapping of these branches results in the coexistence of two periodic attractors (generalized bistability) and the coexistence of multiple periodic attractors (generalized multistability). Regular SNBs may cause various kinds of crises[3,14]

Many researchers have theoretically and experimentally investigated the complex dynamics, such as generalized bistability and multistability in pump-modulated EDFLs, over a wide range of the modulation parameters.[4,5,7] Luo *et al*[6] and Sungchul Kim *et al*,[15] reported chaos and chaotic synchronization of the loss-modulated erbium-doped fibre-ring lasers (EDFRLs) but they did not study the bifurcation structures corresponding to the nonlinear response of the laser system which were numerically investigated in a Fabry–Perot cavity laser subjected to the modulated loss at the high-frequency range where the modulation frequency is higher than the relaxation oscillation frequency of the laser.[3] In this paper we demonstrate a systematic experimental investigation of the characteristics of the bifurcation structure in the lower modulation frequency range ($f_m < f_r/2$) in a loss-modulated EDFRL. The complex dynamic behaviours are observed with the modulation frequency as the control parameter.

2. Farey tree and devil's staircase in the loss-modulated EDFRL

The experimental setup of the loss-modulated EDFL is shown in Fig.1. The gain device is an erbium-doped fiber amplifier (EDFA) consisting of a piece of

†Corresponding author. E-mail: liuyue02@mails.thu.edu.cn

25-m long EDF pumped by a 980-nm pump-laser and an isolator. In all the experimental results shown below, the pump power is fixed at 85 mW. A band-pass filter composed of a fiber Bragg grating (FBG) and an optical circulator is inserted into the cavity. The FBG has a reflectivity of 90% at 1546.7-nm and a 3-dB bandwidth of 0.2 nm. The polarization in the cavity is adjusted by a polarization controller (PC). A pair of AOMs with the opposite frequency shift (±27 MHz) is used as the loss modulation device. The external modulation signal (S) is added on AOM1 which shifts the optical frequency from ν_0 to ν_0+27 MHz to realize harmonic modulation of the cavity loss, while AOM2 works in CW mode to eliminate the self-pulsing caused by the frequency-shifted feedback of the AOM.[16] Their place can be exchanged without affecting the results of the experiments. The signal voltage applied to the AOM driver is

$$S(t) = V_{\rm b}\left[1 + m_i \sin\left(2\pi f_{\rm m} t\right)\right], \qquad (1)$$

where $V_{\rm b}$ is the bias voltage and equals 438 mV in our experiments, $m_i = V_{\rm m}/V_{\rm b}$ ($V_{\rm m}$ is the driving voltage amplitude) and $f_{\rm m}$ are the modulation index and the modulation frequency, respectively. In our experiment, m_i is equal to 3.65%. The laser light is divided by a fiber coupler with a coupling ratio of 80:20. The total cavity length is 57 m and the relaxation oscillation frequency ($f_{\rm r}$) of the laser is about 22 kHz. The laser's temporal output is measured by a photodetector (PD, Agilent 83440B) with a bandwidth of 6 GHz and an oscilloscope (OSC, Agilent 54833A) with a bandwidth of 1 GHz. The power spectrum of the temporal output can be analyzed by using the fast Fourier transformation function of the OSC.

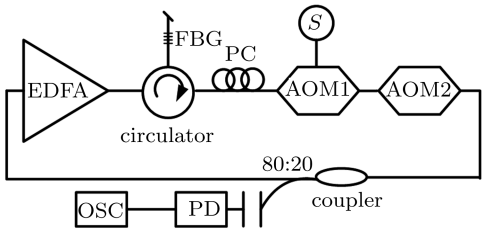


Fig.1. The experimental setup of the unidirectional EDFRL.

The typical output time series of the laser are shown in Fig.2, with the corresponding modulation signals in the same figure (upper lines). In Fig.2(a) one modulation cycle produces one lasing pulse, whereas in Fig.2(b) one modulation cycle produces two lasing

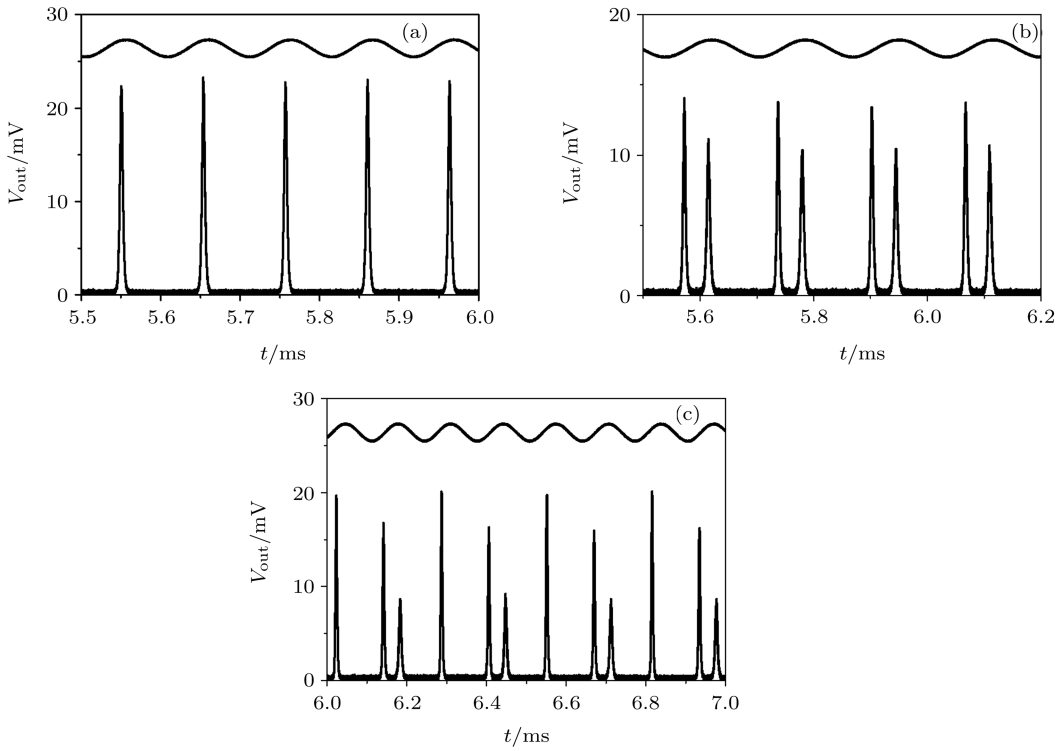


Fig.2. The corresponding time series for different winding numbers: (a) $f_{\rm m} = 9680$ Hz, $w = 1/1$; (b) $f_{\rm m} = 6058$ Hz, $w = 1/2$; (c) $f_{\rm m} = 7573$ Hz, $w = 2/3$. The output curve is the lower line belonging to the left axis, while the modulation signal is the upper line in each figure in Figs.2, 5 and 7.

pulses. In Fig.2(c) the period of the output time trace is twice that of the modulation signal, while three pulses in two modulation cycles make Fig.2(c) look like a compound of Figs.2(a) and 2(b). Each periodic state represents a particular attractor. There are two important numbers for each periodic attractor: the period number m and the pulse number n. The period number m is defined as the quotient of the period of the periodic attractor divided by the period of the modulation. It is a natural number. When $m = 1$ the resulting oscillation is of the same period as the modulation, and when $m = 2$ the period of the resulting oscillation is twice that of the modulation, and so on. Each attractor with $m > 1$ is the subharmonic branch of the modulation signal of order m, or generally called the period-m attractor. The periodic attractor tends to a chaotic or strange attractor when m goes to infinity. The pulse number n is the number of peaks (maxima of the curve) in m periods and shows the resonances between $f_{\rm m}$ and $f_{\rm r}$. Since a pair of m and n, namely (m, n), clearly denotes a particular attractor, we further define a "winding number" as

$$w = m/n. \tag{2}$$

Thus we can identify different periodic attractors with their winding number, e.g. $w = 1/1$, $1/2$ and $2/3$ for those shown in Figs.2(a), 2(b) and 2(c), respectively.

As the modulation frequency is slowly increased and decreased, various stable time series with certain values of w can be shown in the screen of the OSC. The winding numbers can be predicted by a pure Farey-tree construction which is first reported in a modulated external-cavity semiconductor laser.[17]

In Fig.3 the winding number as a function of the modulation frequency yields the upper fractal curve called a devil's staircase. The winding numbers appear from left to right in the order obtained by the Farey tree. Between two winding numbers m/n and m'/n' one can find another one with w=$(m+m')/(n+n')$, e.g. $2/3 = (1+1)/(1+2)$, as is identified in the figure. In our experiment, we have detected the periodic states expected according to the Farey tree up to an order of $m = 6$ between $w = 1/2$ and $w = 1$. The gaps between the stairs refer to the quasi-periodicity, or in some regions, chaos.[14] The width of the range for the frequency ratio which gives a stable m/n periodic state depends on the level m/n where the hierarchy of the Farey tree appears. In addition, we show in Fig.3 the bifurcation diagram of the maximum amplitude of laser pulses, i.e. $V_{\rm out}$ for the same modulation frequencies. Since the period-1 attractor with $w = 1$ exists in the range around half of the relaxation frequency, we focus on the dynamics in the low-frequency range ($f_{\rm m} < f_{\rm r}/2$). A comparison with the upper curve reveals that there exist fine structures of bifurcation in some stairs because of the multiple values at certain frequencies. Period-doubling phenomena are found at $w = 1/4$ and some other stairs. The overlapping of the stair 1/4 and the stair 1/5 indicates a bistability in the corresponding frequency range. And more complex bifurcations display at the stair 1/3.

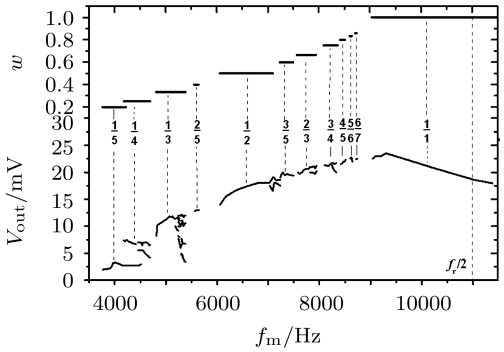


Fig.3. Measured winding numbers (upper curve belonging to the upper part of left axis) and peaks of the output time series (lower curve belonging to the lower part of left axis) as a function of the modulation frequency $f_{\rm m}$. The half of the relaxation frequency, $f_{\rm r}/2(\approx 11$ kHz) is shown by the vertical dashed line.

3. The coexistence of two and more attractors (generalized bistability and generalized multistability)

In this section, we will investigate the details of the period doubling and coexistence of multiple attractors which are displayed in Fig.3 at lower values of the winding numbers. The bifurcation diagram at $w = 1/4$ and $w = 1/5$ is shown in Fig.4 and that at $w = 1/3$ is shown in Fig.6. Labels P_n^m and R_n^m appear in the diagrams constructed by slowly increasing and decreasing $f_{\rm m}$ respectively. In Refs.[3] and [4], label P refers to the state of the large-amplitude spikes while label R refers to the state of the small-amplitude almost-sinusoidal trace. The former and the latter represent the nonlinear response and the regular linear response of the laser system, respectively. Here, we use the labels P_n^m and R_n^m to label different kinds of attractors, where m and n are the period number and the pulse number, respectively. So

the corresponding periodic attractors of the time series shown in Figs.2(a), 2(b) and 2(c) are P_1^1, P_2^1 and P_3^2 in turns.

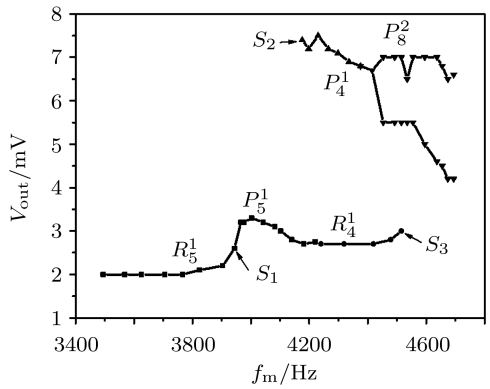


Fig.4. A bifurcation diagram of the loss-modulated EDFRL with modulation frequency ($f_{\rm m}$) as a control parameter.

In Fig.4 generalized bistability, i.e., the coexistence of two attractors with the same winding number but with different amplitudes, has been found within a certain frequency range at w=1/4. The R_4^1 attractor dies in the subcritical SNB (S_3), while the P_4^1 attractor arises in the supercritical SNB (S_2). The time series of the R_4^1 and P_4^1 attractors at the same modulation frequency are shown in Fig.5(c). The former is found to be much smaller in amplitude than the latter. There is a continuous degeneration from the R_4^1 attractor to the P_5^1 attractor. Under the conditions of the experiment, the subcritical SNB (S_1) of the R_5^1 attractor has been found, but we do not find the exact SNB point where the P_5^1 attractor is born. At a slightly higher level of the modulation amplitude, the supercritical SNB of P_5^1 attractor and generalized bistability of the attractors with $w = 1/5$ can be observed (not shown). The SNB points labeled S_i ($i = 1$, 2, 3) are marked by the arrows in the diagram. The time series corresponding to the R_5^1 and P_5^1 attractors are shown in the Figs.5(a) and 5(b), which clearly display the difference between the R attractors and the P attractors. As $f_{\rm m}$ is increased, a period-2 P_8^2 attractor appears as the consequence of period doubling of the P_4^1 attractors (see Fig.5(d)). Period doubling is also found in the stairs 1/2, 2/3 and 3/4. When $f_{\rm m}$ comes into the gap between the stairs 1/4 and 1/3, chaos appears from the temporal dynamics.

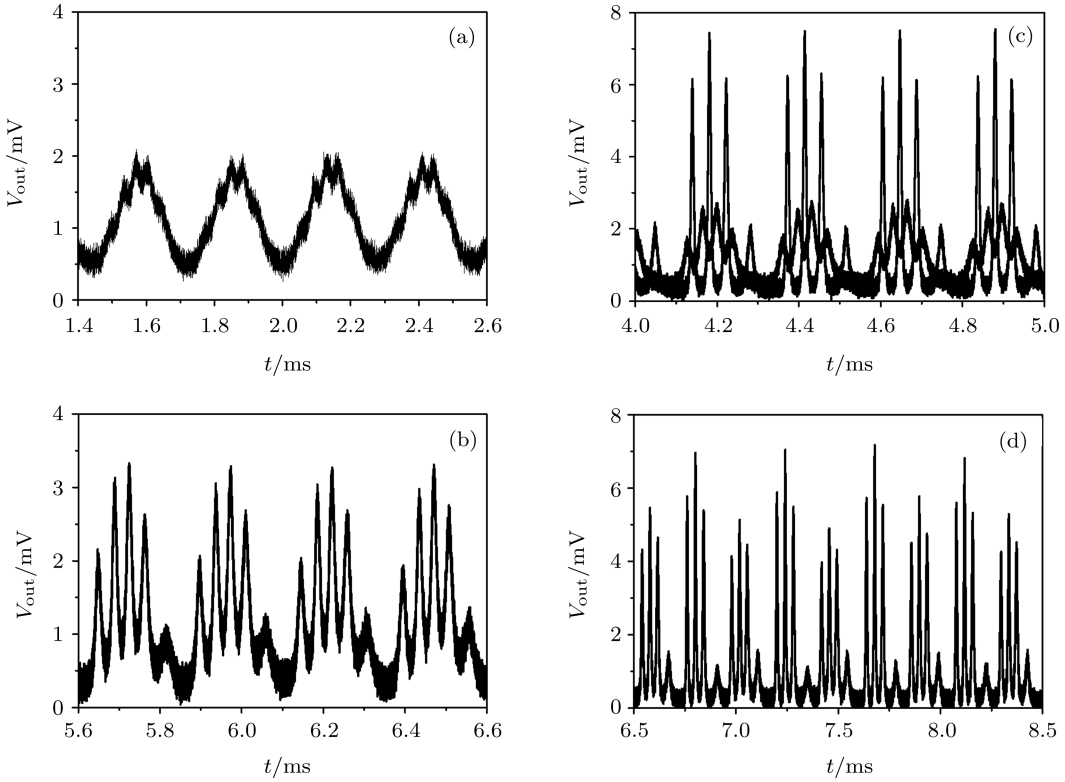


Fig.5. A time series corresponding to the dynamics shown in Fig.4 for different modulation frequencies: (a) $f_{\rm m}$ = 3620 Hz, R_5^1; (b) $f_{\rm m}$ = 4000 Hz, P_5^1; (c) $f_{\rm m}$ = 4300 Hz, R_4^1 and P_4^1; (d) $f_{\rm m}$ = 4555 Hz, P_8^2, period 2 of P_4^1. The sinusoidal curves show the modulation signal.

A type of crisis appears at $f_{\rm m} = 4816$ Hz in Fig.6, where the instantaneous disappearance of the chaotic attractor and its basin of attraction is observed. Crises are caused by a collision between a chaotic attractor and an unstable point or periodic orbit. When the unstable periodic orbit is just at the boundary of the basin of attraction, the crisis is called a boundary crisis.[14,18] In Fig.6 one can see that the chaotic attractor and its basin of attraction are simultaneously destroyed by the boundary crisis and a new periodic attractor P_3^1 is born. The transient behaviour has also been shown in Figs.7(a) and 7(b) in comparison with the time series at $f_{\rm m} = 4816$ Hz and $f_{\rm m} = 4833$ Hz. This kind of crisis was observed earlier in a CO_2 laser[18] with loss modulation and numerically demonstrated in a loss-modulated EDFL[3] with the loss modulation index as the control parameter.

In Fig.6, as $f_{\rm m}$ is increased, the attractors from the period-1 state (P_3^1) to period-4 state (P_{12}^4) born and dead in SNBs appear in turns. The period-doubling subharmonic branch (labeled $P_{12}^{4'}$ with an arrow) of the P_6^2 attractor is found and the corresponding time series of the P_6^2 and $P_{12}^{4'}$ attractors are shown in Figs.7(c) and 7(d). There is also a regular period-1 R_3^1 attractor like the R_4^1 attractor and the P_5^1 attractor originating from the linear response of the system to the parameter modulation. A rich variety of bifurcations of multiple attractors results in generalized multistability. For example, the coexistence of three different dynamical regimes, period-1(R_3^1), period-3(P_9^3) and period-4(P_{12}^4) attractors, is indicated by a dash

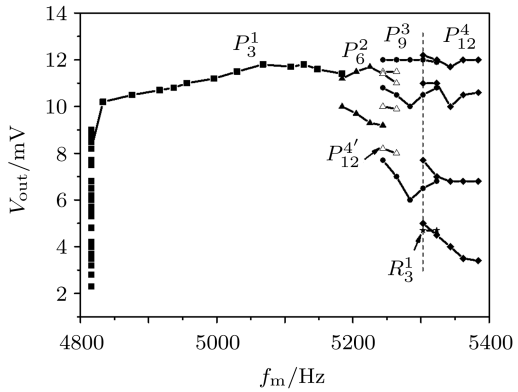
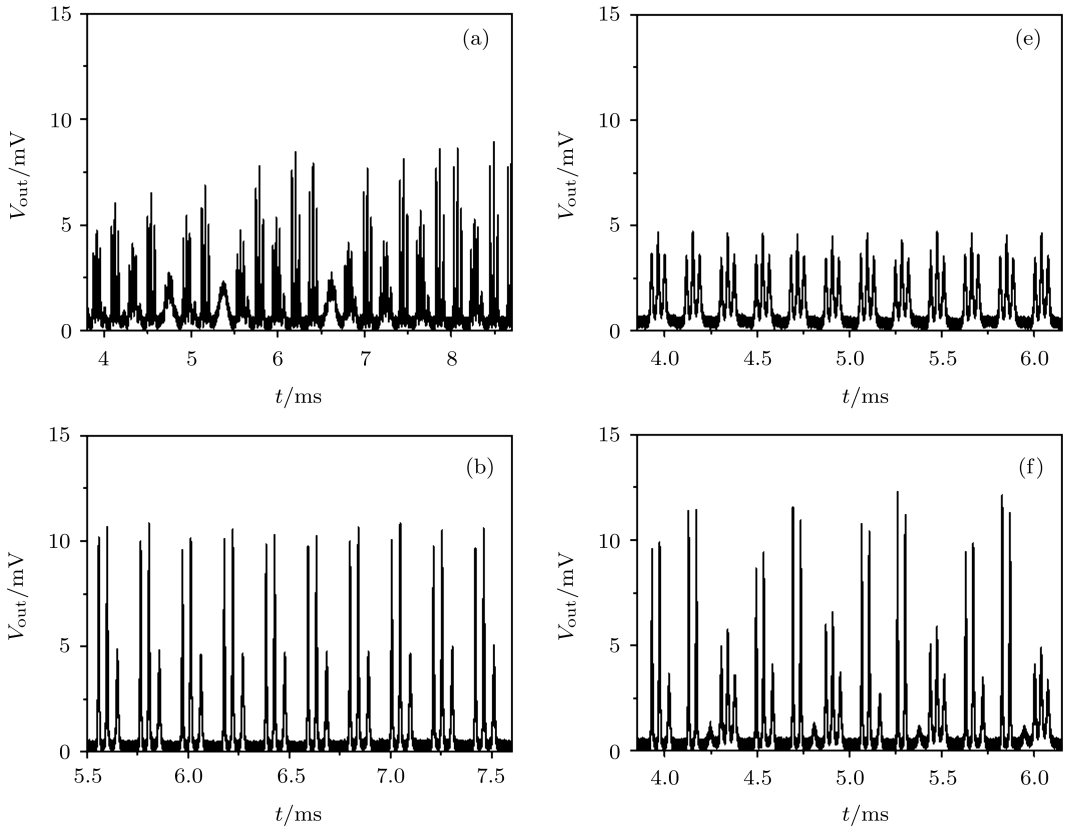


Fig.6. Bifurcation diagram of the loss-modulated EDFRL with modulation frequency ($f_{\rm m}$) as a control parameter. The vertical dashed line indicates the frequency at the time series in Figs.7(e), 7(f) and 7(g).



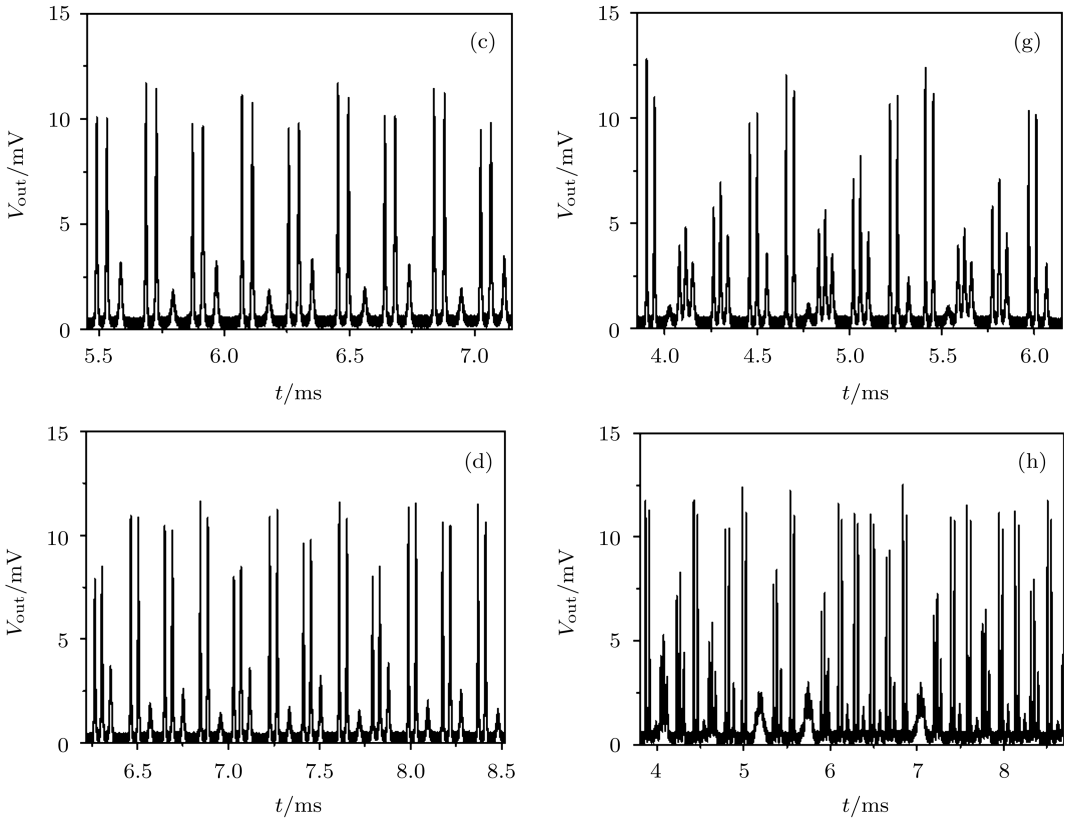


Fig.7. A time series corresponding to the dynamics shown in Fig.6 for different modulation frequencies: (a) $f_{\rm m}$ = 4816 Hz, chaos; (b) $f_{\rm m}$ = 4833 Hz, period 1 of P state, $w = 1/3$; (c) $f_{\rm m}$ = 5205 Hz, period 2 of P state, $w = 1/3$; (d) $f_{\rm m}$ = 5244 Hz, period 4 of P' state, $w = 1/3$; (e) $f_{\rm m}$ = 5303 Hz, period 1 of R state, $w = 1/3$; (f) $f_{\rm m}$ = 5303 Hz, period 3 of P state, $w = 1/3$; (g) $f_{\rm m}$ = 5303 Hz, period 4 of P state, $w = 1/3$; (h) $f_{\rm m}$ = 5386 Hz, chaos. The sinusoidal curves show the modulation signals.

line in Fig.6 and demonstrated with the time series in Figs.7(e), 7(f) and 7(g). These attractors have the same winding number $w = 1/3$ but different period numbers. It is interesting to find that the structures of bifurcation and the coexistence of different periodic attractors in a narrow frequency range are very similar to the results shown in other EDFL systems in a high-frequency range ($f_{\rm m} > f_{\rm r}/2$).[3−5] We guess that it is a consequence of the structural similarity of the bifurcation in a chaotic system. For other values of w, similar results may be achieved with certain modulation parameters. When $f_{\rm m}$ is beyond the right boundary of the bifurcation diagram, the output of the system becomes chaos while the time series is shown in the Fig.7(h).

One can see that the modulation frequency at the measured SNB point where the P_3^1 attractor is born is 50% lower than the predicted frequency $f_{\rm r}/3$. But for $w = 1/5$ the modulation frequency at the SNB point is about 4 kHz which is very close to $f_{\rm r}/5$. The difference is because of the increase of the nonlinearity of the system along with the increase of the parameter $f_{\rm m}$.[4]

4. Conclusion

In conclusion, we have experimentally investigated in detail the dynamics of an EDFRL with loss modulation. The winding numbers of the periodic attractors form a devil's staircase and are obtained by a Farey tree construction. A rich variety of bifurcations including the coexistence of multiple attractors and boundary crisis caused by SNB have been demonstrated in the low-frequency region. An interesting substructure of bifurcations with the modulation frequency as the control parameter has been observed. A further study on the bifurcations in the parameter space with modulation amplitude and modulation frequency will explore more details of the dynamical behaviours in the loss-modulated EDFRLs.

References

[1] Michel J F D 2001 *Rare-Earth-Doped Fibre Lasers and Amplifiers* (New York: Marcel Dekker)

[2] Weiss C O 1991 *Dynamics of Lasers* (Weinheim: VCH)

[3] Saucedo-Solorio J M, Pisarchik A N, Kir'yanov A V and Aboites V 2003 *J. Opt. Soc. Am.* B **20** 490

[4] Pisarchik A N, Barmenkov Y O and Kir'yanov A V 2003 *IEEE J. Quantum Elect.* **12** 1567

[5] Pisarchik A N, Kir'yanov A V and Barmenkov Y O 2005 *J. Opt. Soc. Am.* B **22** 2107

[6] Luo L G and Chu P L 1998 *J. Opt. Soc. Am.* B **15** 2524

[7] Luo L G, Tee T J and Chu P L 1998 *J. Opt. Soc. Am.* B **15** 972

[8] Fan W H, Tian X J, Chen J F, Zheng F, Yu Y L, Gao B and Luo H E 2007 *Chin. Phys.* **16** 2908

[9] Wang R and Shen K 2002 *Phys. Rev.* E **65** 16207

[10] Zhang S H and Shen K 2003 *Chin. Phys.* **12** 149

[11] Sanchez F and Stephan G 1996 *Phys. Rev.* E **53** 2110

[12] Arecchi F T, Meucci R, Puccioni G and Tredicce J 1982 *Phys. Rev. Lett.* **49** 1217

[13] Eschenazi E, Solari H G and Gilmore R 1989 *Phys. Rev.* A **39** 2609

[14] Ott E 1993 *Chaos in Dynamical Systems* (Cambridge: Cambridge University Press UK)

[15] Kim S, Lee B and Kim D H 2001 *IEEE Phon. Tech. Lett.* **13** 290

[16] Maran J, Besnard P and LaRochelle S 2006 *J. Opt. Soc. Am.* B **23** 1302

[17] Baums D, Elsässer W and Göbel E O 1989 *Phys. Rev. Lett.* **63** 155

[18] Lauterborn W and Steinhoff R 1988 *J. Opt. Soc. Am.* B **5** 1097

[19] Dangoisse D, Glorieux P and Hennequin D 1986 *Phys. Rev. Lett.* **57** 2657